

## Original Article

# $^{64}\text{CuCl}_2$ PET/CT imaging of mouse muscular injury induced by electroporation

Fang Xie<sup>1</sup>, Huawei Cai<sup>1,3</sup>, Fangyu Peng<sup>1,2</sup>

<sup>1</sup>Department of Radiology, <sup>2</sup>Advanced Imaging Research Center, University of Texas Southwestern Medical Center, Dallas, TX, USA; <sup>3</sup>Department of Nuclear Medicine, West China Hospital, Sichuan University, Chengdu, Sichuan, China

Received September 28, 2016; Accepted December 9, 2016; Epub January 15, 2017; Published January 30, 2017

**Abstract:** Skeletal muscle injury is common in body injuries suffered in sports and car accidents. Development of new tracers is significant for assessing muscular injury with positron emission tomography/computed tomography (PET/CT) and monitoring repair of muscle injury in response to treatment. Copper is required for wound healing and increased copper ions were detected in the soft tissue of wound in rodents and human. Based on the recent finding of increased  $^{64}\text{Cu}$  uptake in the traumatic brain injury, this study aimed to explore use of  $^{64}\text{CuCl}_2$  as a radiotracer for molecular imaging of muscular injury using PET/CT. Focally increased  $^{64}\text{Cu}$  uptake by the injured muscular tissue ( $5.4 \pm 1.2\%$  ID/g) was detected in the C57BL/6 mice with electroporation-induced skeletal muscle injury by PET/CT after intravenous injection of  $^{64}\text{CuCl}_2$  as a tracer, compared to low  $^{64}\text{Cu}$  uptake associated with muscular inflammation induced by intramuscular injection of lipopolysaccharides ( $0.82 \pm 0.26\%$  ID/g,  $P < 0.01$ ) or physiological  $^{64}\text{Cu}$  uptake of the non-injured muscular tissues ( $0.78 \pm 0.20\%$  ID/g,  $P < 0.01$ ). The findings support further investigation of  $^{64}\text{CuCl}_2$  as a new radiotracer for molecular imaging of skeletal muscle injury using PET/CT.

**Keywords:** Muscle injury, electroporation, positron emission tomography, copper metabolism, copper-64 chloride

## Introduction

Skeletal muscle injury is very common in athletes, like soccer, basketball, and kickboxing players who suffered traumatic injury during sport events. It is caused by excessive force or stress on the muscle. Muscle injury caused pain and impaired performance which may prevent or delay their return to competitions [1]. Inconvenience and discomfort associated with such injuries caused a significant economic impact in athletes and also in workers. Skeletal muscle injury can also be caused by other work-related trauma or car accidents, contraction, chemicals, myotoxins, electric shocks and ischemia [2-5].

Imaging techniques are increasingly being used to assess skeletal muscle injury in athletes [3, 5, 6]. Image modalities such as ultrasound or magnetic resonance imaging (MRI) have been used to assess location, extent, and severity of acute muscle injuries, which assists in making assumptions regarding prognosis and timing of

return to sports [3, 5-8]. There were attempts to use PET/CT for assessment of metabolic changes associated with muscle injury. PET studies of thermally injured muscle have been previously reported using 2-[ $^{18}\text{F}$ ]fluoro-2-deoxy-D-glucose ([ $^{18}\text{F}$ ] FDG) [9]. It was found that the thermally injured muscle showed a decrease in [ $^{18}\text{F}$ ] FDG uptake as compared to normal tissues. In view of physiological background of muscular [ $^{18}\text{F}$ ] FDG uptake, it is significant to search new tracers for noninvasive assessment of muscle injury with PET/CT.

Copper plays a critical role for many aspects of cellular growth and metabolism in mammals, including brain development, respiration, peptide hormone production, and cellular proliferation and tumor growth [10, 11]. Copper metabolism is regulated by a delicate network of copper transporters [12, 13]. It has been known that copper is required for repair of wound [14, 15]. Increased  $^{64}\text{Cu}$  uptake by traumatized brain tissue in mice was detected by PET/CT after intravenous injection of copper (II)-64 chloride

( $^{64}\text{CuCl}_2$ ) as a tracer for assessment of traumatic brain injury (TBI) [16]. Intense  $^{64}\text{Cu}$  radioactivity was also visualized at craniotomy site in mice subjected to controlled cortical impact (CCI) for induction of TBI [16]. The aim of this pilot study was to explore  $^{64}\text{CuCl}_2$  as a new tracer for molecular imaging of muscular injury using PET/CT.

### Materials and methods

#### *Reagents, radiopharmaceuticals and animals*

Lipopolysaccharides (LPS) was purchased from Sigma-Aldrich (Saint Louis, MO). The radiopharmaceutical,  $^{64}\text{CuCl}_2$ , was purchased from Mallinckrodt Institute of Radiology, Washington University School of Medicine. Balb/c mice (8 weeks, female,  $n = 10$ ) were purchased from animal resource center, the University of Texas Southwestern Medical Center (Dallas, TX). Experiments of using small animals in this study were conducted according to the protocol approved by the UT Southwestern Institutional Animal Care and Use Committee.

#### *Induction of muscular injury*

Muscular injury in Balb/c mice ( $n = 5$ ) was induced by electroporation using an electroporator (ECM 830, Harvard apparatus). After injection of 100  $\mu\text{L}$  of PBS to the leg muscles, BTX 2-needle array was inserted into muscles of left leg at 5 mm depth and electroporation was applied to induce muscle injury with a field strength of 180 V/cm (pulse parameter: 90 V, 20 msec per pulse and 8 pulses in total). Intramuscular injection of LPS (100  $\mu\text{g}$ /per injection site) was performed at contralateral right leg to induce muscular inflammation as control.

#### *PET/CT imaging*

PET/CT imaging of mice with electroporation-induced muscular injury on one leg and muscular inflammation induced by LPS on another leg were performed using an Inveon PET/CT scanner (Siemens) as described previously [16-18]. Briefly, the mice were anesthetized by inhalation of 3% isoflurane in 100% oxygen (3 L/min) at room temperature after 5 days of electroporation or injection of LPS and imaged at 0.5, 2 and 24 hours after intravenous injection of  $^{64}\text{CuCl}_2$  (2  $\mu\text{Ci/g}$  body weight) via the tail vein. The dose of  $^{64}\text{CuCl}_2$  (2  $\mu\text{Ci/g}$  body weight) selected for this study was based on the dose of  $^{64}\text{CuCl}_2$  used in previous PET/CT imaging of

traumatic brain injury [16] and copper metabolism disorders in *Atp7b*<sup>-/-</sup> knockout mouse model of Wilson disease [17]. PET data was reconstructed using measured attenuation, scatter correction, and the ordered subsets expectation maximization (OSEM) 3D iterative algorithm, yielding an isotropic spatial resolution of about 2 mm full width at half maximum [19]. The images were subsequently processed and the Regions of interests (ROIs) of the muscle injury site and contralateral thigh muscle were drawn on PET/CT images. PET quantitative analysis was performed to obtain decay-corrected percentage of injected dose per gram of tissue (% ID/g) for each ROI using Inveon Research Workplace (IRW) software (Siemens) as described previously [16-18].

#### *Histological analysis of muscular tissue*

Upon completion of PET/CT imaging, the mice were euthanized under anesthesia and post-mortem mouse tissues including injured muscle and contralateral control tissues were harvested for histological tissue analysis. The muscle sections were fixed in 10% NBF, embedded in paraffin, and cut in 5  $\mu\text{m}$  sections. The sections were then stained with hematoxylin and eosin (H&E). Microscopic images of the stained sections were recorded with an Olympus microscope equipped with a Spot digital camera (Diagnostic Instruments, Sterling Heights, MI).

#### *Statistical analysis*

Statistical analysis of PET data was performed with data of quantitative PET analysis (% ID/g) expressed as mean  $\pm$  standard deviation (SD). In order to determine whether tracer uptake observed using PET/CT imaging (% ID/g) differed significantly between injured muscle and non-injured muscle or muscular tissue with LPS-induced inflammation, paired t test was performed. A *P*-value of less than 0.05 was considered to represent statistical significance.

### Results

#### *Visualization of increased $^{64}\text{Cu}$ uptake by injured muscle on PET/CT images*

$^{64}\text{CuCl}_2$  PET/CT imaging of the mice ( $n = 5$ ) with muscular injury (left leg) and inflammation (right leg) was performed to evaluate muscular

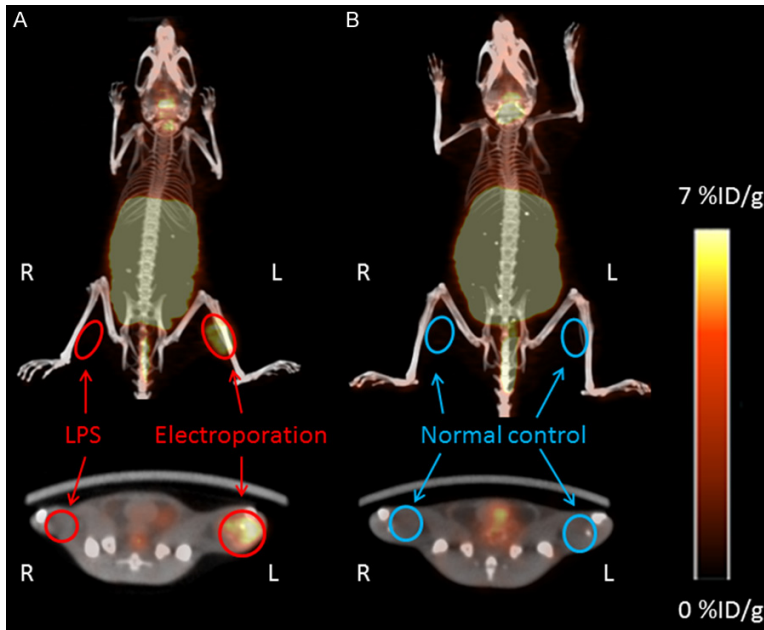


**Figure 1.** PET/CT imaging of mouse muscular injury induced by electroporation at 2 hours after injection of  $^{64}\text{CuCl}_2$  as a radiotracer. A. Increased  $^{64}\text{Cu}$  uptake by the injured muscular tissue in mice subjected to electroporation on left leg was visualized on PET/CT images, in contrast to low  $^{64}\text{Cu}$  uptake in the muscular tissue of contralateral right leg with inflammation induced by LPS injection. B. Low background  $^{64}\text{Cu}$  radioactivity in the muscular tissue of bilateral legs of normal control mouse. LPS, lipopolysaccharides; R, right; L, left; % ID/g, percentage of injected dose per gram.

intestine of the mice, in contrast to low  $^{64}\text{Cu}$  radioactivity in the brain after intravenous injection of  $^{64}\text{CuCl}_2$  (**Figure 1**; **Table 1**). The whole body biodistribution of  $^{64}\text{Cu}$  in mice injected with  $^{64}\text{CuCl}_2$  intravenously was similar to the whole body biodistribution of  $^{64}\text{Cu}$  in C57BL/6 mice injected with  $^{64}\text{CuCl}_2$  as described previously [17]. Focally increased  $^{64}\text{Cu}$  uptake by the electroporation-injured muscular tissue was visualized in the left leg of the mice (**Figure 1A**), compared to low  $^{64}\text{Cu}$  uptake in the muscular tissue of contralateral right leg injected with LPS (**Figure 1A**), and background  $^{64}\text{Cu}$  uptake of non-injured muscle on the bilateral legs of control mice (**Figure 1B**).

*PET quantification of increased  $^{64}\text{Cu}$  uptake by electroporation-injured muscular tissue*

**Table 1.** Biodistribution of  $^{64}\text{Cu}$  radioactivity and muscular  $^{64}\text{Cu}$  uptake in mice with electroporation-induced muscle injury (left leg) and LPS-induced muscular inflammation (right leg) by PET/CT after intravenous injection of  $^{64}\text{CuCl}_2$  as a radiotracer

	0.5 h*	2 h	24 h
Liver	14.6 ± 3.8**	15.9 ± 2.9	11.2 ± 0.57
Heart	2.2 ± 0.63	1.85 ± 0.49	2.0 ± 0.36
Muscle	0.90 ± 0.29	0.78 ± 0.20	0.58 ± 0.11
Brain	0.58 ± 0.07	0.50 ± 0.03	0.75 ± 0.13
Kidney	7.6 ± 2.8	5.2 ± 1.4	3.6 ± 0.52
Lung	3.0 ± 0.53	2.1 ± 0.45	2.2 ± 0.50
Muscle injury	4.8 ± 1.8	5.4 ± 0.45	2.9 ± 0.60
Inflammation	0.84 ± 0.25	0.82 ± 0.26	0.91 ± 0.33

\*h, hour; \*\*% ID/g, percentage of injected dose per gram.

There was increased  $^{64}\text{Cu}$  uptake by the injured muscle compared with  $^{64}\text{Cu}$  uptake by the muscular tissue with inflammation induced by LPS and background muscular  $^{64}\text{Cu}$  uptake in the mice without injury (**Table 1**). At 2 hour post injection,  $^{64}\text{Cu}$  uptake by the injured muscle on the left leg was measured at  $5.4 \pm 1.2\%$  ID/g, compared with low  $^{64}\text{Cu}$  uptake by the muscle with inflammation induced by LPS on the right leg ( $0.82 \pm 0.26\%$  ID/g,  $P < 0.01$ ), or physiological muscular  $^{64}\text{Cu}$  uptake in the bilateral legs of control mice ( $0.78 \pm 0.20\%$  ID/g,  $P < 0.01$ ). The ratio of  $^{64}\text{Cu}$  uptake by the injured muscle to background  $^{64}\text{Cu}$  uptake by the non-injured muscle was 7.2 at 2 h post injection. There was no significant difference of muscular  $^{64}\text{Cu}$  radioactivity in the right leg injected with LPS ( $0.82 \pm 0.26\%$  ID/g) compared with muscular  $^{64}\text{Cu}$  radioactivity in the bilateral legs of the mice without injury or inflammation induced by LPS ( $0.78 \pm 0.20\%$  ID/g,  $P > 0.5$ ) at 2 hour post injection of the tracer. PET quantitative analysis has also revealed time-dependent changes of  $^{64}\text{Cu}$  uptake by the muscular tissue injured by electroporation, showing interval decrease

$^{64}\text{Cu}$  uptake after intravenous injection of  $^{64}\text{CuCl}_2$  as a tracer. Additionally,  $^{64}\text{CuCl}_2$  PET/CT imaging of the mice (n = 5) without muscular injury was performed as normal control. On the whole body PET/CT images, there was abundant  $^{64}\text{Cu}$  radiotracer uptake in the liver and

## $^{64}\text{CuCl}_2$ PET/CT of muscular injury

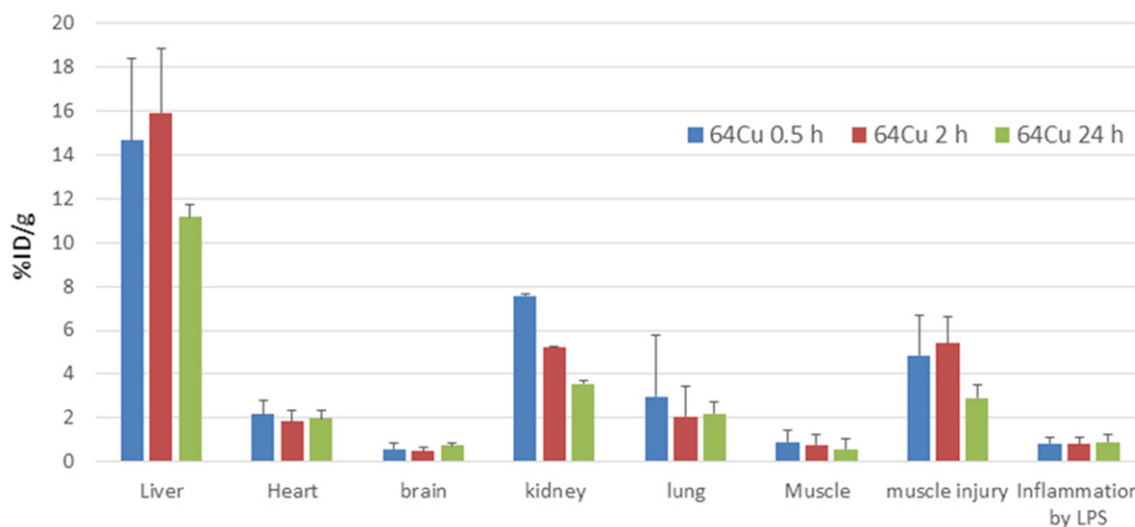


**Figure 2.** PET quantification of  $^{64}\text{Cu}$  radioactivity and increased  $^{64}\text{Cu}$  uptake by muscular tissue injured by electroporation. Abundant  $^{64}\text{Cu}$  radioactivity was present in the liver, in contrast to low physiologic  $^{64}\text{Cu}$  radioactivity in the brain and non-injured muscle. Increased  $^{64}\text{Cu}$  uptake by injured muscular tissue reached peak at 2 hour post injection, which has decreased by 24 hour post injection, but still significantly higher than  $^{64}\text{Cu}$  uptake by the muscular tissue with inflammation induced by LPS and low background  $^{64}\text{Cu}$  uptake by the non-injured muscular tissue. h, hour; LPS, lipopolysaccharides; % ID/g, percentage of injected dose per gram.

from  $5.4 \pm 1.2\%$  ID/g at 2 hours post injection to  $2.9 \pm 0.6\%$  ID/g at 24 hour post injection (Figures 2, 3).

### Histological analysis of muscular tissue

In contrast to normal morphology of non-injured muscular tissue, morphological changes of injured muscular tissue from the mice subjected to electroporation was demonstrated by histological analysis, showing muscle degeneration, fragmentation, and necrosis on H&E stained tissues slides by microscopic examination (Figure 3B), corresponding to increased  $^{64}\text{Cu}$  uptake by PET quantification (Figure 3A). In contrast, there was only minimal increase of  $^{64}\text{Cu}$  uptake by the muscular tissue with inflammation induced by LPS (Figure 3A), despite infiltration of muscular tissue by large number of inflammatory cells and macrophagocytosis following injection of LPS, as visualized on H&E stained tissue slides by microscopic examination (Figure 3B).

### Discussion

In this pilot study, increased  $^{64}\text{Cu}$  uptake by the injured muscle was demonstrated in mice by PET/CT after intravenous injection of  $^{64}\text{CuCl}_2$  as a tracer. To the best of our knowledge, this is a

first report of increased  $^{64}\text{Cu}$  uptake by injured muscular tissues in mice assessed by PET/CT imaging after intravenous injection of  $^{64}\text{CuCl}_2$  as a tracer.

Molecular mechanism of increased  $^{64}\text{Cu}$  uptake in the injured muscular tissue remains to be elucidated, which might be related to increased demand of copper for functional activity of cellular enzymes essential for wound healing process, as suggested by previous findings of increased copper concentration in wound fluid or tissue [14, 15]. It was reported that there was change of copper concentration in inflammation tissue [20, 21]. We compared  $^{64}\text{Cu}$  uptake by the muscular tissue injured by electroporation with  $^{64}\text{Cu}$  uptake by the muscular tissue with inflammation induced by LPS. We found that there was only minimal increase of  $^{64}\text{Cu}$  uptake by the muscular tissue with LPS-induced inflammation, in contrast to significantly increased  $^{64}\text{Cu}$  uptake by the electroporation-injured muscular tissue (Figures 1-3; Table 1). These findings suggested that increased  $^{64}\text{Cu}$  radioactivity localized at site of muscular injury was likely due to increased flow of copper to injured muscular tissue, not increased copper uptake by the inflammatory cells associated with post-injury muscular inflammation. If injury-specific increase of  $^{64}\text{Cu}$  uptake is con-

### $^{64}\text{CuCl}_2$ PET/CT of muscular injury

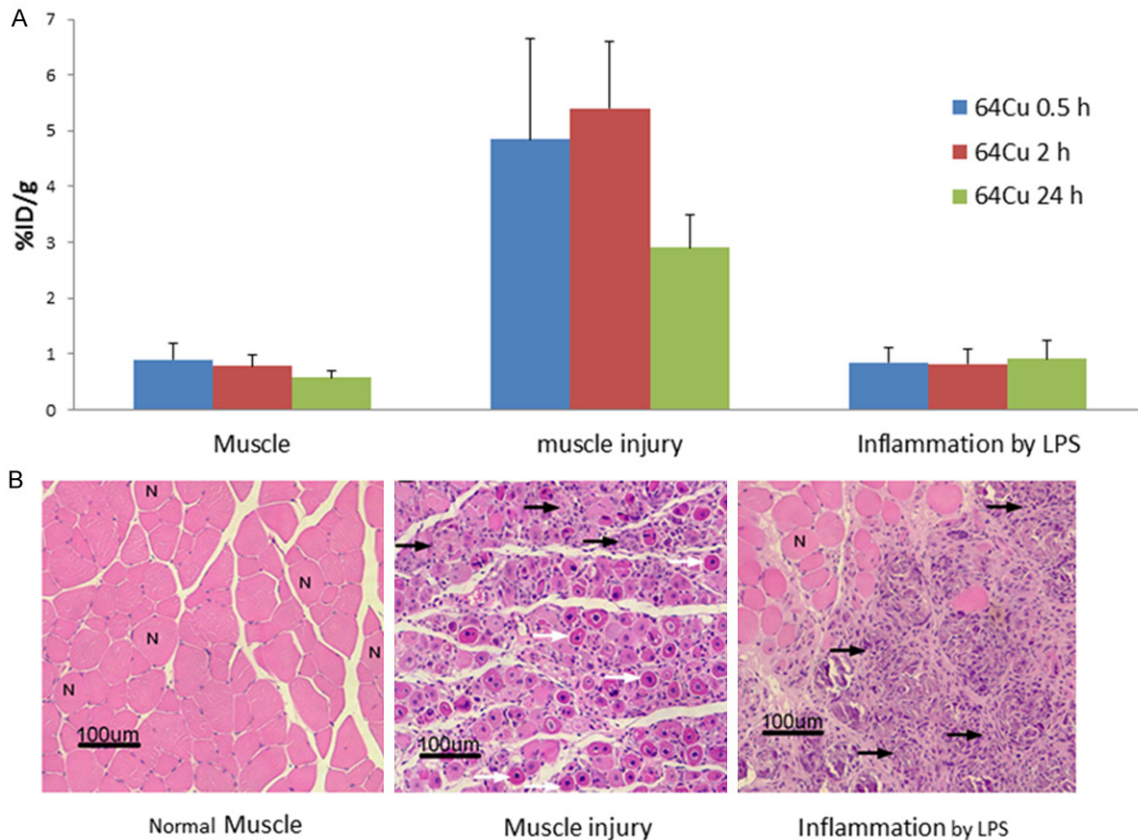


**Figure 3.** Correlation of  $^{64}\text{Cu}$  uptake on PET/CT with histological analysis of postmortem mouse muscular tissues. A. Increased  $^{64}\text{Cu}$  uptake by injured muscular tissues in mice with muscular injury caused by electroporation quantified by PET/CT after intravenous injection of  $^{64}\text{CuCl}_2$ , compared with low  $^{64}\text{Cu}$  uptake by muscular inflammation induced by LPS and background  $^{64}\text{Cu}$  uptake by non-injured muscular tissues. B. Microscopic imaging of H&E stained postmortem mouse muscular tissue. Photo on left: non-injured mouse muscle showing normal morphology of myofibers (N denotes normal). Photo at middle: Muscular tissue injured by electroporation, showing degeneration and necrosis of myofibers and macrophagocytosis (highlighted by black arrows) with regenerating cells indicated by centrally located nuclei (highlighted by white arrows). Photo on right: Muscular tissue with inflammatory cell infiltration induced by LPS. h, hour; LPS, lipopolysaccharides; % ID/g, percentage of injected dose per gram.

firmed by further investigation in human study,  $^{64}\text{CuCl}_2$  will be a promising new tracer for molecular imaging of muscle injury using PET/CT. In this pilot study, electroporation was used to induce muscular injury in mice as a mouse model of muscular injury based on previous use of electroporation for muscular gene delivery and potential use of different parameters of electroporation to control severity and extent of muscle injury. Additional studies are necessary to test use of  $^{64}\text{CuCl}_2$ -PET/CT for assessment of muscle injuries caused by a mechanical force or other methods.

Focally increased  $^{64}\text{Cu}$  uptake detected by PET (Figure 1) was correlated with microscopic findings of degeneration and necrosis of myofibers

and macrophagocytosis induced by electroporation (Figure 3). Additional studies are necessary to determine increased  $^{64}\text{Cu}$  uptake of muscular injury at cellular level using autoradiography, in view of limited spatial resolution of PET/CT imaging. Additionally, high-performance liquid chromatography inductively coupled plasma mass spectrometry (LC-ICP-MS) may be used to delineate molecules bound with  $^{64}\text{Cu}$  in the blood of the mice injected with  $^{64}\text{CuCl}_2$  and determine whether increased  $^{64}\text{Cu}$  radioactivity in the injured muscle represent free  $^{64}\text{Cu}$  bound with cellular component of muscle fibers or deposition of  $^{64}\text{Cu}$  bound macromolecules from blood due to enhanced permeability and retention (EPR) effect induced by electroporation. Moreover, it remains to be

determined whether increased flow of copper to wound tissue is related to body response to oxidative stress associated with muscle injury.

In comparison to other imaging modalities, such as ultrasound and MRI, clinical application of <sup>64</sup>CuCl<sub>2</sub>-PET/CT for diagnostic imaging of acute muscular injury may be limited by high cost, local availability, and exposure to radiation. However, <sup>64</sup>CuCl<sub>2</sub>-PET/CT may be useful as a tool for evaluation of extent of chronic muscular injury based on its high sensitivity for metabolic imaging when findings of ultrasound and MRI are equivocal in extent of delayed repair of muscle injury. Despite its common occurrence, treatments for muscular injuries, such as ice compresses, NSAIDs or muscle relaxers, were sometimes not effective and surgery may need to remove injured muscular tissue for extreme cases [22, 23]. There is a need of imaging tool to assess response of injured muscular tissue to treatment in order to determine the time when athletes are ready to return to sport competition. In addition to its potential use for diagnostic imaging of muscular injury, it will be interesting to conduct a longitudinal <sup>64</sup>CuCl<sub>2</sub>-PET/CT to monitor time-dependent changes of <sup>64</sup>Cu accumulation post muscular injury and explore potential use of <sup>64</sup>CuCl<sub>2</sub>-PET/CT as a tool for monitoring repair of injured muscular tissue in response to treatment. This new <sup>64</sup>CuCl<sub>2</sub>-PET/CT technology may play a role in development of new medications or therapeutic approaches for better treatment of muscular injury.

### Conclusion

Focally increased <sup>64</sup>Cu uptake by muscular tissue injured by electroporation was detected in mice with PET/CT after intravenous injection of <sup>64</sup>CuCl<sub>2</sub> as a tracer, supporting further investigation of <sup>64</sup>CuCl<sub>2</sub> as a new tracer for PET/CT imaging of skeletal muscle injury.

### Acknowledgements

We acknowledge assistance from Rachel Sparks in mouse tissue histological analysis. This pilot study was partially supported by NIH (7R21EB005331-03 and 1R21NS074394-01A1 to FP). The production of <sup>64</sup>CuCl<sub>2</sub> at Washington University School of Medicine was supported by NIH/NCI (R24 CA86307).

### Disclosure of conflict of interest

None.

**Address correspondence to:** Dr. Fangyu Peng, Department of Radiology, University of Texas Southwestern Medical Center, 5323 Harry Hines Blvd, Dallas 75390, Texas, USA. Tel: 214-645-2625; Fax: 214-645-6479; E-mail: Fangyu.Peng@UTSouthwestern.edu

### References

- [1] Ekstrand J, Healy JC, Walden M, Lee JC, English B and Hagglund M. Hamstring muscle injuries in professional football: the correlation of MRI findings with return to play. *Br J Sports Med* 2012; 46: 112-117.
- [2] Lu H, Huang D, Ransohoff RM and Zhou L. Acute skeletal muscle injury: CCL2 expression by both monocytes and injured muscle is required for repair. *FASEB J* 2011; 25: 3344-3355.
- [3] Slavotinek JP. Muscle injury: the role of imaging in prognostic assignment and monitoring of muscle repair. *Semin Musculoskelet Radiol* 2010; 14: 194-200.
- [4] Koulouris G and Connell D. Hamstring muscle complex: an imaging review. *Radiographics* 2005; 25: 571-586.
- [5] Speer KP, Lohnes J and Garrett WE Jr. Radiographic imaging of muscle strain injury. *Am J Sports Med* 1993; 21: 89-96.
- [6] May DA, Disler DG, Jones EA, Balkissoon AA and Manaster BJ. Abnormal signal intensity in skeletal muscle at MR imaging: patterns, pearls, and pitfalls. *Radiographics* 2000; 20: S295-315.
- [7] Connell DA, Schneider-Kolsky ME, Hoving JL, Malara F, Buchbinder R, Koulouris G, Burke F and Bass C. Longitudinal study comparing sonographic and MRI assessments of acute and healing hamstring injuries. *Am J Roentgenol* 2004; 183: 975-984.
- [8] Koulouris G, Connell DA, Brukner P and Schneider-Kolsky M. Magnetic resonance imaging parameters for assessing risk of recurrent hamstring injuries in elite athletes. *Am J Sports Med* 2007; 35: 1500-1506.
- [9] Carter EA, Tompkins RG, Hsu H, Christian B, Alpert NM, Weise S and Fischman AJ. Metabolic alterations in muscle of thermally injured rabbits, measured by positron emission tomography. *Life Sci* 1997; 61: 39-44.
- [10] Olivares M and Uauy R. Copper as an essential nutrient. *Am J Clin Nutr* 1996; 63: 791S.
- [11] Uauy R, Olivares M, Gonzalez M. Essentiality of copper in humans. *Am J Clin Nutr* 1998; 67: 952S-959S.
- [12] Puig S and Thiele DJ. Molecular mechanisms of copper uptake and distribution. *Curr Opin Chem Biol* 2002; 6: 171-180.

## $^{64}\text{CuCl}_2$ PET/CT of muscular injury

- [13] Lutsenko S. Human copper homeostasis: a network of interconnected pathways. *Curr Opin Chem Biol* 2010; 14: 211-217.
- [14] Jones PW, Taylor DM and Williams DR. Analysis and chemical speciation of copper and zinc in wound fluid. *J Inorg Biochem* 2000; 81: 1-10.
- [15] Lansdown AB, Sampson B and Rowe A. Sequential changes in trace metal, metallothionein and calmodulin concentrations in healing skin wounds. *J Anat* 1999; 195: 375-386.
- [16] Peng F, Muzik O, Gatson J, Kernie SG and Diaz-Arrastia R. Assessment of traumatic brain injury by increased  $^{64}\text{Cu}$  uptake on  $^{64}\text{CuCl}_2$  PET/CT. *J Nucl Med* 2015; 56: 1252-1257.
- [17] Peng F, Lutsenko S, Sun X and Muzik O. Positron emission tomography of copper metabolism in the *Atp7b*<sup>-/-</sup> knock-out mouse model of Wilson's disease. *Mol Imaging Biol* 2012; 14: 70-78.
- [18] Peng F, Lutsenko S, Sun X and Muzik O. Imaging copper metabolism imbalance in *Atp7b*<sup>-/-</sup> knockout mouse model of Wilson's disease with PET-CT and orally administered  $^{64}\text{CuCl}_2$ . *Mol Imaging Biol* 2012; 14: 600-607.
- [19] Hudson HM and Larkin RS. Accelerated image reconstruction using ordered subsets of projection data. *IEEE Trans Med Imaging* 1994; 13: 601-609.
- [20] Milanino R, Marrella M, Gasperini R, Pasqualicchio M and Velo G. Copper and zinc body levels in inflammation: an overview of the data obtained from animal and human studies. *Agents Actions* 1993; 39: 195-209.
- [21] Whitehouse MW and Walker WR. Copper and inflammation. *Agents Actions* 1978; 8: 85-90.
- [22] Heiderscheit BC, Sherry MA, Silder A, Chumanov ES and Thelen DG. Hamstring strain injuries: recommendations for diagnosis, rehabilitation, and injury prevention. *J Orthop Sports Phys Ther* 2010; 40: 67-81.
- [23] Maffulli N, Del Buono A, Oliva F, Giai Via A, Frizziero A, Barazzuol M, Brancaccio P, Freschi M, Galletti S, Lisitano G, Melegati G, Nanni G, Pasta G, Ramponi C, Rizzo D, Testa V, Valent A. Muscle injuries: a brief guide to classification and management. *Transl Med UniSa* 2014; 12: 14-8.